Prediction of differential work-hardening behavior under biaxial tension of steel sheet using crystal plasticity models

Hama, Takayuki; Fujimoto, Hitoshi; Takuda, Hirohiko

Available online at www.sciencedirect.com

ScienceDirect

Procedia Manufacturing 15 (2018) 1808–1815

Procedia MANUFACTURING

www.elsevier.com/locate/procedia

17th International Conference on Metal Forming, Metal Forming 2018, 16-19 September 2018, Toyohashi, Japan

Prediction of differential work-hardening behavior under biaxial tension of steel sheet using crystal plasticity models

Takayuki Hama*, Hitoshi Fujimoto, Hirohiko Takuda

Department of Energy Science and Technology, Kyoto University, Yoshida-honmachi, Sakyo-ku, Kyoto 606-8501, Japn

Abstract

Evolution of plastic contour of a steel sheet was predicted using various crystal plasticity models, including a phenomenological and dislocation-based hardening model. The evolution of plastic contour was different depending on the model, but none of the models used could predict differential work-hardening behavior observed in experiments. The simulation results showed that the {110} and {112} slip activities were significantly different depending on the stress ratio, suggesting that the differences in the strengths between the {110} and {112} slip systems would play an important role in the evolution of the contour.

Peer-review under responsibility of the scientific committee of the 17th International Conference on Metal Forming.

Keywords: Contour of equal plastic work; Steel sheet; Crystal plasticity; Dislocation density; Interaction matrix

1. Introduction

Recently, crystal plasticity models are receiving much attention because of their ability to predict various macroscopic deformation behaviors, such as work hardening under uniaxial and multiaxial loadings and evolution of Lankford value, from the mesoscopic deformation. These models are nowadays utilized for various metals. Concerning work-hardening behavior under biaxial tension, evolution of contour of equal plastic work was predicted successfully using crystal plasticity models for face-centered cubic and hexagonal close-packed metals. Yoshida et al. [1] studied the predictive accuracy of evolution of contour of equal plastic work of a 3000 series aluminum alloy sheet and reported that a phenomenological-hardening model did not give any differential work-hardening, while a

* Corresponding author. Tel.: +81-75-753-5418; fax: +81-75-753-5428.
E-mail address: hama@energy.kyoto-u.ac.jp

2351-9789
Peer-review under responsibility of the scientific committee of the 17th International Conference on Metal Forming.
10.1016/j.promfg.2018.07.210

dislocation-density based model yielded differential work-hardening similar to experimental results. They presumed that the differential work-hardening could be predicted by using a dislocation-density based model because the difference in the evolution of dislocation density depending on the stress ratio was properly taken into account. Hama et al. [2, 3] predicted evolutions of contour of equal plastic work of a magnesium alloy and commercially pure titanium sheet by using a crystal plasticity model with good accuracy. They also explained that the strong differential work-hardening occurred in these sheets because active slip and twinning systems were different depending on the stress ratio.

In contrast, the predictive accuracy of contour of equal plastic work for body-centered cubic metals, especially for steels, is still poor [4, 5]. For instance, Jeong et al. [4] predicted the evolution of plastic contours of an interstitial-free steel sheet using a viscoplastic self-consistent crystal plasticity model, but the simulation could not reproduce the differential work-hardening observed in experimental results. One of the reasons that the predictive accuracy for body-centered cubic metals is poor would be that crystal plasticity modelling for body-centered cubic metals is still insufficient and needs further improvement. For instance, in body-centered cubic metals, it was reported that the {110} and {112} slip systems were active, but the critical resolved shear stress could be different between the two slip systems, and the critical resolved shear stress for the {112} slip systems could be different between the twinning and antitwinning directions [6]. Furthermore, latent hardening is not understood well [7, 8], and sometimes Schmid law does not hold [9, 10]. Although various crystal plasticity models have been proposed to predict the work-hardening behavior of steels [4, 5], the predictive accuracy is still insufficient as mentioned earlier, and moreover, the effect of crystal plasticity modelling on the predictive accuracy is not understood well. In the present study, evolution of contour of equal plastic work of a steel sheet was predicted using various crystal plasticity models, and the effect of crystal plasticity modelling on the predictive accuracy was systematically investigated.

2. Crystal plasticity models

The {110} and {112} slip systems of body-centered cubic structure were taken into consideration. The slip activity was modeled by using the following crystal plasticity models.

2.1. Accumulated-slip based hardening model (model A)

Following Hoc et al. [11], the slip rate $\dot{\gamma}^{\alpha}$ of the α slip system was given in the form

$$\dot{\gamma}^{\alpha}=\begin{cases}\dot{\gamma}_0\left(\dfrac{\left|\tau^{\alpha}\right|-\tau_Y^{\alpha}}{\tau_0}\right)^{\frac{1}{m}}\operatorname{sgn}\left(\tau^{\alpha}\right) & \text{if } \left|\tau^{\alpha}\right|>\tau_Y^{\alpha}\\ 0 & \text{if } \left|\tau^{\alpha}\right|\le\tau_Y^{\alpha}\end{cases}, \tag{1}$$

where $\dot{\gamma}_0$ is the reference-strain rate, m is the rate-sensitivity exponent, τ^{α} is the resolved shear stress, τ_0 is the initial strength, and τ_Y^{α} is the slip resistance. The evolution of τ_Y^{α} was given as $\dot{\tau}_Y^{\alpha}=\sum_{\beta}h_{\alpha\beta}\left|\dot{\gamma}^{\beta}\right|$, where $h_{\alpha\beta}$ denotes the hardening matrix. The work-hardening rate was phenomenologically given as a function of accumulated slip as

$$h_{\alpha\beta}=q_{\alpha\beta}h_0\left(\frac{h_0\bar{\gamma}}{\tau_0 n}+1\right)^{n-1},\quad \bar{\gamma}=\sum_{\alpha}\int_0^t\left|\dot{\gamma}^{\alpha}\right|, \tag{2}$$

where n, and h_0 are the material parameters. $q_{\alpha\beta}$ is the latent hardening matrix.

2.2. Dislocation-density based hardening model (model D)

Eq. (1) was used to represent the slip rate also in this model. The work-hardening rate was given as a function of dislocation density in the form [12]

$$h_{\alpha\beta} = g_{\alpha\beta}\frac{\mu}{2}\left(\sum_{\kappa} g_{\alpha\kappa}\rho^{\kappa}\right)^{-\frac{1}{2}}\left\{\frac{1}{L^{\beta}} - 2y_c\rho^{\beta}\right\}, \quad L^{\alpha} = K\left(\sum_{\kappa} g_{\alpha\kappa}\rho^{\kappa}\right)^{-\frac{1}{2}}, \quad \dot{\rho}^{\alpha} = \frac{1}{b}\left(\frac{1}{L^{\alpha}} - 2y_c\rho^{\alpha}\right)\left|\dot{\gamma}^{\alpha}\right|, \tag{3}$$

where K is the material parameter. b and y_c are the magnitude of Burgers vector and the characteristic length related to the annihilation process of dislocation dipoles, respectively. μ is the shear modulus. $g_{\alpha\beta}$ is the dislocation interaction matrix. ρ^{α} is the dislocation density, and its initial value is ρ_0.

2.3. Peeters model (model P)

A model proposed by Peeters et al. [13] was used. In this model, the dislocation substructure was presumed to consist of the development of cell-block boundaries and cell boundaries, which were associated with latent and isotropic hardening, respectively. τ_Y^{α} was given as

$$\tau_{\mathrm{Y}}^{\alpha} = \tau_0 + (1-f)\tau^{CB} + f\tau_{\alpha}^{CBB}, \tag{4}$$

where τ^{CB} and τ_{α}^{CBB} are the resistances due to cell boundaries and cell-block boundaries on the α-slip system, respectively. f is the volume fraction. τ_{α}^{CBB} is assumed to be given as a function of the densities of immobile dislocations stored in cell block boundaries and directionally movable dislocations stored at a side of cell block boundaries, whereas τ^{CB} is given as a function of the statistically stored dislocation density in the cell interiors. The characteristic point of this model compared to the models A and D is that latent hardening, which is modeled by using τ_{α}^{CBB}, is given as a function of the dislocation densities. For the detail formulation of Peeters model, refer to literature [13].

The abovementioned models were incorporated into our in-house crystal plasticity finite-element method program [14]. It should be noted that the model P was used in its rate form because our program was on the basis of the rate form of the principle of virtual work [15].

2.4 Parameter identification

A cubic model with ten uniform divisions in each direction was used as the representative volume element. Eight-node solid elements with selective reduced integration were utilized. A cold-rolled steel sheet was assumed in this study. The initial pole figure is shown in Fig. 1. The same initial orientation was assigned to all the eight integration points in each element. The material parameters were determined to fit the stress-strain curve under uniaxial tension. The components of $q_{\alpha\beta}$ in eq. (2) (model A) were set to be unity. On the other hand, to examine the

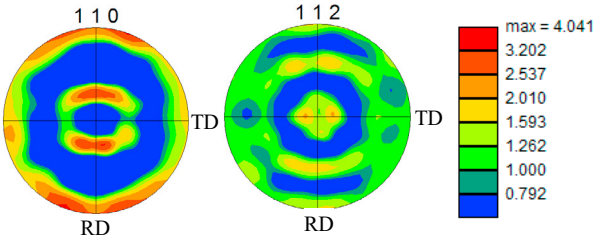

Fig. 1. Initial pole figures of material assumed in simulation.

effect of interaction matrix, two sets of parameters were used for $g_{\alpha\beta}$ in the model D: all the components were set to be unity in the first set (model D1), whereas the parameters shown in Table 1 determined on the basis of literature [7, 8] were used in the second set (model D2). The determined material parameters for the models A, D1, D2, and P are shown in Tables 2, 3, and 4. The simulation procedure of biaxial tension was the same as that of literature [2, 3]. The simulation was conducted for the conditions of σ_{xx}: σ_{yy} =1:0, 6:1, 3:1, 2:1, 1.5:1, 1:1, 1:1.5, 1:2, 1:3, 1:6, and 0:1, where x and y denote respectively the rolling and transverse directions.

Table 1. Parameters of interaction matrix for model D2 [7, 8]. Refer to the cited literature for the meaning of the variables.

h(1)	h(2)	h(3)	h(4)	h(5)	h(6)	h(7)	h(8)	h(9)
0.1	0.1	0.45	5.5	0.4	0.6	5.5	0.1	0.1
h(10)	h(11)	h(12)	h(13)	h(14)	h(15)	h(16)	h(17)	
5.5	0.1	0.1	0.1	0.1	0.1	0.1	0.1	

Table 2. Hardening parameters for model A.

τ_0 /MPa	h_0 /MPa	n
45.0	965	0.3

Table 3. Hardening parameters for models D1 and D2.

τ_0 /MPa	ρ_0 /mm^{-2}	K	y_c(mm)	b /mm
45.0	2.73 x 10^5	30.0 (Model D1) 10.0 (Model D2)	1.65 x 10^{-3}	2.48 x 10^{-7}

Table 4. Hardening parameters for model P. Refer to literature [13] for meaning of variables.

τ_0 /MPa	f	α	K^{wd}	y_c^{wd} /mm	K^{wp}
45.0	0.20	0.15	1.00	1.70×10^{-5}	8.00
y_c^{wp} /mm	y_c^{neg} /mm	y_c^{rev} /mm	K	y_c /mm	y_c^{rev2} /mm
3.50×10^{-6}	3.50×10^{-6}	1.00×10^{-5}	15.0	5.70×10^{-7}	1.00×10^{-6}

3. Results and discussion

In the following, the contours of equal plastic work were normalized by using the stress obtained with σ_{xx}: σ_{yy} =1:0, σ_0, at each plastic work, W_0. Fig. 2(a) shows examples of experimental results of the normalized contours of plastic work at different W_0. The normalized contour gradually expanded with the increase of plastic work, and the expansion was more pronounced for the conditions $\sigma_{xx} \geq \sigma_{yy}$. This result is consistent with that reported by Nakano et al. [16]. The predictive accuracy of the simulation results are discussed on the basis of this experimental result.

Figs. 2(b) – 2(e) show the normalized contours of plastic work predicted at different W_0 by using the aforementioned models. When the model A was used (Fig. 2(b)), the change in the normalized contour was negligibly small. When the model D1 (Fig. 2(c)) was used, the overall change in the contour was larger than that of the model A. The contour in the vicinity of σ_{xx}: σ_{yy} =2:1 remained unchanged to W_0 = 2 /MJ*m^{-3} and then expanded. In contrast, the contour at equibiaxial tension remained unchanged throughout the process, as in the case of the model A. When the model D2 was used (Fig. 2(d)), the contour shrank rapidly to W_0 = 4 /MJ*m^{-3} and then slightly expanded. Although the tendency of the change was completely opposite from that of the experiment, the differential work-hardening was the largest among the models. When the model P was used (Fig. 2(e)), the tendency was different depending on the stress ratio. At equibiaxial tension, the contour rapidly shrank to W_0 = 2 /MJ*m^{-3} and then slightly expanded. On the other hand, in the vicinity of σ_{xx}: σ_{yy} =2:1, the contour remained unchanged to W_0 = 1 /MJ*m^{-3}, and then slightly expanded.

The abovementioned simulation results showed that the evolution of contour of equal plastic work differed depending on the crystal plasticity model and that none of the models used could properly predict the expanding tendency of the normalized contour observed in the experiments. Comparing the results among the models, the differential hardening is more pronounced in the dislocation-density based models D1, D2, and P than in the accumulated-slip based model A. This result is consistent with that of an aluminum alloy sheet reported in Yoshida

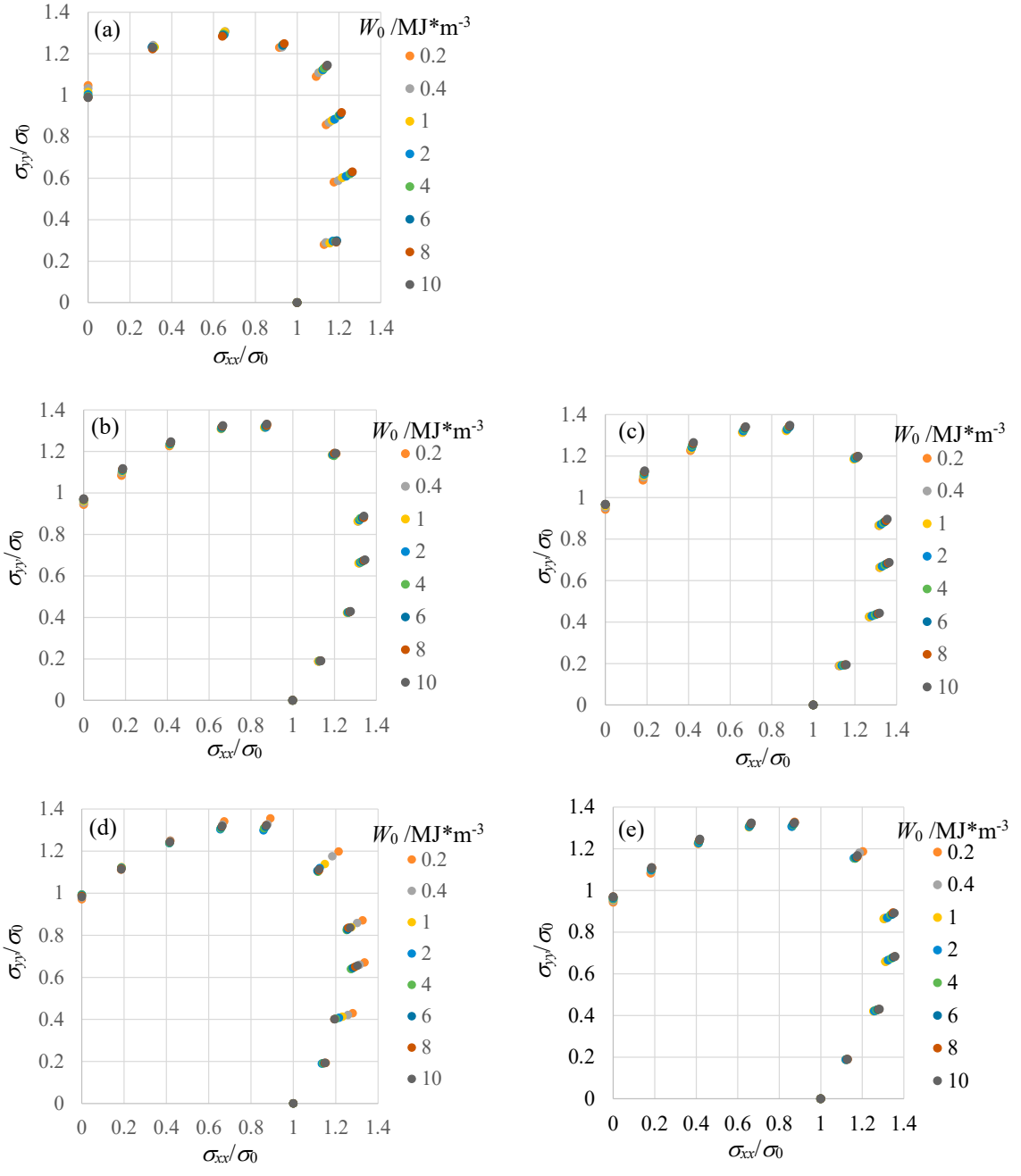

Fig. 2. Contours of equal plastic work. (a) Experiment, (b) model A, (c) model D1, (d) model D2 and (e) model P.

et al. [1]. Concerning the effect of dislocation interaction matrix, it is likely that the anisotropic properties in the matrix components yield large differential hardening in the normalized contour (the model D2). Moreover, the effect of the difference in the dislocation interaction matrix on the simulation result (the difference between the models D1 and D2) is much more pronounced than that of the difference in the hardening model (the difference between the models A and D1). In contrast, although the latent hardening was taken into account in the model P, the degree of differential hardening was rather similar to that of the model D1.

To examine the deformation mechanism, the evolution of relative activities of the {110} and {112} slip systems at different stress ratios in the case of the model D1 is shown in Fig. 3. At σ_{xx}: σ_{yy} =1:0, the activity of {110} slip systems was larger than that of the {112} slip systems. However, the activity of the {112} slip systems increased as the stress ratio approached σ_{xx}: σ_{yy} =1:1, and eventually, the activity of the {112} slip systems was dominant at σ_{xx}: σ_{yy} =1:1. This result was almost independent of the model. The aforementioned results suggest that the predictive accuracy of the differential hardening would be improved if the effect of the difference between the {110} and {112} slip activities on the work-hardening is properly taken into account. Indeed, as explained in the introduction, it has been reported that the critical resolved shear stresses and work-hardening would be different between the {110} and {112} slip systems. For instance, Franciosi et al. [6] recently reported that the critical resolved shear stress of the {110} slip systems might be approximately equal to that of the {112} slip systems in the twinning direction and was smaller than that of the {112} slip systems in the antitwinning direction. Moreover, they also reported that the work-hardening of the {110} slip systems might be larger than that of the {112} slip systems in the twinning direction and smaller than that of the {112} slip systems in the antitwinning direction.

On the basis of the abovementioned observations, the effect of the difference in the critical resolved shear stresses between the {110} and {112} slip systems on the differential hardening was numerically examined. To simplify the problem, the difference in the properties between the twinning and antitwinning direction was not taken into account and we just assigned larger critical resolved shear stress for the {112} slip systems ($\tau_0^{\{112\}}$ =60 MPa) than those of the {110} slip systems ($\tau_0^{\{110\}}$ = 45 MPa). The result obtained using the model D1 is shown in Fig. 4. Although the normalized contour slightly shrank to W_0 = 1 /MJ*m^{-3}, thereafter it expanded irrespective of the stress ratio, consistent with the experimental result. The aforementioned result suggests that it may be important to take the differences in the critical resolved shear stress, and presumably work-hardening as well, between the {110} and {112} slip systems to improve the predictive accuracy of the evolution of plastic contour of this material.

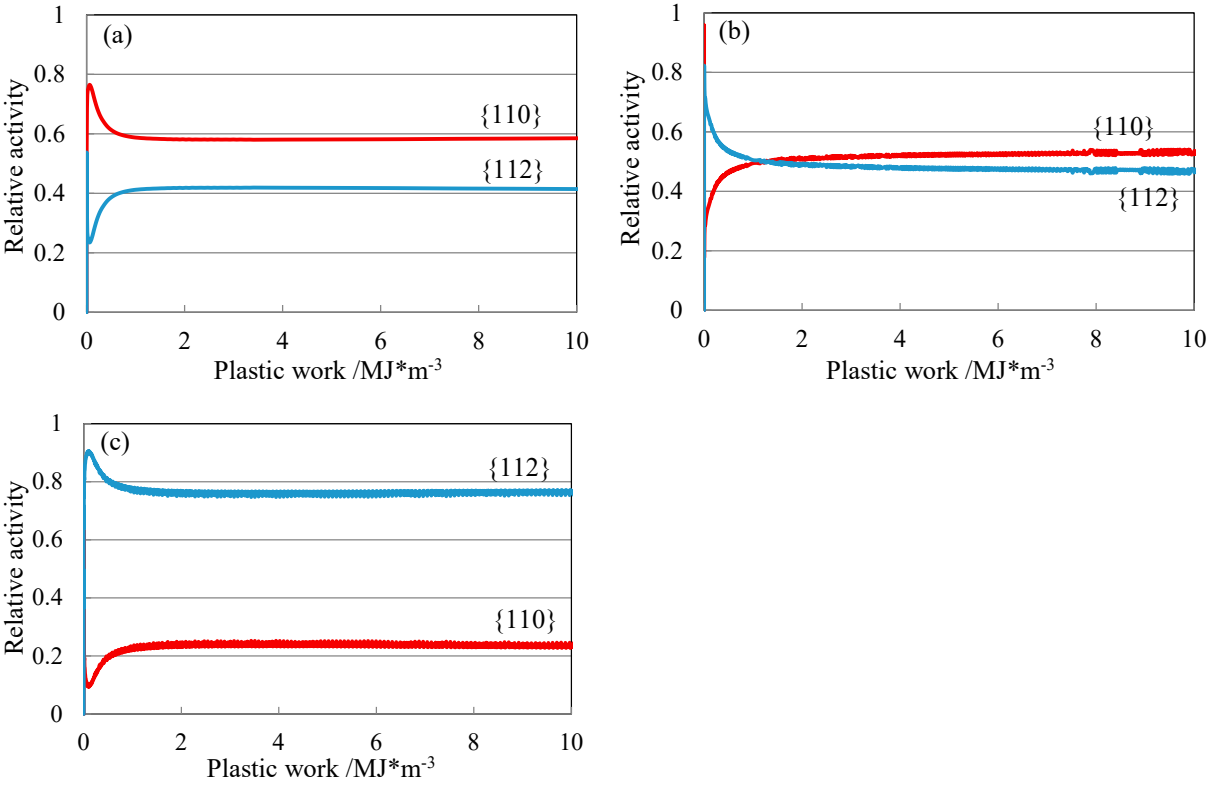

Fig. 3. Evolution of relative activities during biaxial tension obtained using model D1. σ_{xx}: σ_{yy} = (a) 1:0, (b) 2:1, and (c) 1:1.

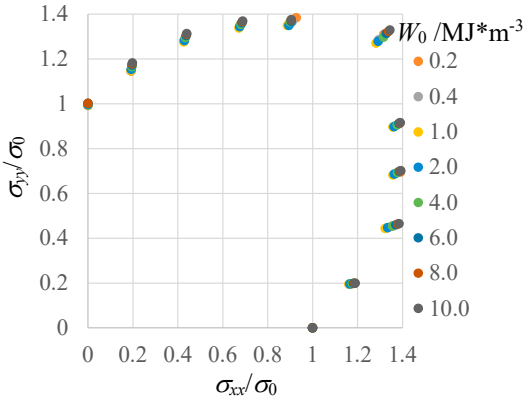

Fig. 4. Simulated contours of equal plastic work by using the model D1 with larger critical resolved shear stress for the {112} slip systems than for the {110} slip systems.

4. Conclusion

In the present study, evolution of contour of equal plastic work of a cold-rolled steel sheet was predicted using various crystal plasticity models, and the effect of crystal plasticity modelling on the predictive accuracy was discussed. The results obtained in this study are summarized as follows.

(1) The evolution of plastic contour is different depending on the crystal plasticity model: the normalized contour remains almost unchanged regardless of the plastic work when the accumulated-slip based hardening model is used, while the normalized contour expands slightly when the dislocation-density based hardening models are used. When the dislocation-density based model with the interaction matrix determined by Madec and Kubin [7, 8] is used, the contour rapidly shrinks to $W_0 = 2$ /MJ*m^{-3} and then slightly expands. None of the models used can reproduce the expanding trend in the normalized contour observed in the experiment.

(2) The simulation results show that the activities of the {110} and {112} slip systems differ depending on the stress ratio.

(3) The numerical experiments suggest that the difference in the strengths between the {110} and {112} slip systems would play an important role in the evolution of the contour.

Acknowledgements

The experiment was conducted by using the biaxial tensile testing machine transferred from Kuwabara laboratory in Tokyo University of Agriculture and Technology. The help of Mr. Yuya Nakatsuji and Mr. Shogo Yagi of Kyoto University with conducting biaxial tensile tests is acknowledged. This study was partially supported by JSPS KAKENHI Grant numbers 17H03428 and 17K06858, Quantum Basic Research Coordinated Development Program from the Ministry of Education, Culture, Sports, Science and Technology, Japan, and ISIJ research grant.

References

[1] K. Yoshida, A. Ishii, Y. Tadano, Work-hardening behavior of polycrystalline aluminum alloy under multiaxial stress paths, International Journal of Plasticity, 53 (2014) 17–39.

[2] T. Hama, H. Takuda, Crystal plasticity finite-element simulation of work-hardening behavior in a magnesium alloy sheet under biaxial tension, Computational Materials Science, 51 (2012) 156–164.

[3] T. Hama, A. Kobuki, H. Takuda, Crystal-plasticity finite-element analysis of anisotropic deformation behavior in commercially pure titanium Grade 1 sheet, International Journal of Plasticity, 91 (2017) 77–108.

[4] Y. Jeong, M.A. Iadicola, T.G. Herold, A. Creuziger, Multiaxial constitutive behavior of an interstitial-free steel: Measurements through X-ray and digital image correlation, Acta Materialia, 112 (2016) 84–93.

[5] P. Eyckens, H. Mulder, J. Gawad, H. Vegter, D. Roose, T. van den Boogaard, A.V. Bael, P.V. Houtte, The prediction of differential hardening behavior of steels by multi-scale crystal plasticity modelling, International Journal of Plasticity, 73 (2015) 119–141.

[6] P. Franciosi, L.T. Le, G. Monnet, C. Kahloun, M.H. Chavanne, Investigation of slip system activity in iron at room temperature by SEM and AFM in-situ tensile and compression tests of iron single crystals, International Journal of Plasticity, 65 (2015) 226–249.
[7] R. Madec, L.P. Kubin, Dislocation interactions and symmetries in bcc crystals, Proceedings of IUTAM Symposium on Mesoscopic Dynamics of Fracture Process and Materials Strength, Kluwer Academic Publishers, Netherlands, (2004) 69–78.
[8] R. Madec, L.P. Kubin, Disloation dynamics in bcc crystals: Interaction strengths in the athermal regime, Proceedings of 3rd International Conference on Computational Modeling and Simulation of Materials Part A, Techna Group, Faenza, (2004) 671–678.
[9] W.A. Spitzig, R.J. Sober, O. Richmond, Pressure dependence of yielding and associated volume expansion in tempered martensite, Acta Metalurgica, 23 (1975) 885–893.
[10] J.W. Christian, Some surprising features of the plastic deformation of body-centered cubic metals and alloys, Metallurgical Transactions A, 14-7 (1983) 1237–1256.
[11] T. Hoc, S. Forest, Polycrystal modelling of IF-Ti steel under complex loading path, International Journal of Plasticity, 17 (2001) 65–85.
[12] C. Teodosiu, J.L. Raphanel, L. Tabourot, Finite element simulation of the large elastoplastic deformation of multicrystals, Proceedings of the international seminar MECAMAT'91, A.A. Balkema, Rotterdam, (1993) 153–168.
[13] B. Peeters, M. Seefeldt, C. Teodosiu, S.R. Kalidindi, P.V. Houtte, E. Aernoudt, Work-hardening/softening behavior of b.c.c. polycrystals during changing strain paths: I. An integrated model based on substructure and texture evolution, and its prediction of the stress-strain behavior of an IF steel during two-stage strain paths, Acta Materialia, 49 (2001) 1607–1619.
[14] T. Hama, H. Takuda, Crystal-plasticity finite-element analysis of inelastic behavior during unloading in a magnesium alloy sheet, International Journal of Plasticity, 27 (2011) 1072–1092.
[15] T. Hama, K. Kojima, M. Kubo, H. Fujimoto, H. Takuda, Crystal plasticity finite-element simulation on development of dislocation structures in bcc ferritic single crystals, ISIJ International, 57-5 (2017) 866–874.
[16] H. Nakano, K. Ichikawa, T. Kuwabara, Measurement and analysis of differential hardening of a cold rolled mild steel sheet, CAMP-ISIJ, 29 (2016) 243.